Influence of multiatom interactions on the shapes and energetics of two-dimensional homoepitaxial clusters on close-packed metallic surfaces

M. C. Fallis and C. Y. Fong

Department of Physics, University of California, Davis, California 95616

(Received 6 September 1995; revised manuscript received 8 April 1996)

We describe a scheme (BSM for ''bond saturation model'') for modeling the energetics of adatom clusters on close-packed metallic surfaces. In the BSM, atoms interact via *coordination dependent* nearest-neighbor bonds. We show that the BSM yields a detailed understanding of the relationship between shape and energy for two-dimensional (2D) homoepitaxial adatom clusters on close-packed metallic surfaces. In particular, we advance a simple rule for predicting the binding energies of small clusters based on the moments of their coordination distributions, derive a useful expression for the binding energy of a 2D cluster of arbitrary geometry, and study the role played by coordination dependent bonding in determining step energies for adatom islands. Our analysis of step energies provides insight into why the two distinct types of monatomic steps on Pt(111) have similar free energies as observed by Michely and Comsa. While our numerical results are for Pt(111), we expect our conclusions to hold for any chemically similar system. [S0163-1829(96)05740-2]

I. INTRODUCTION

On all metal surfaces the relationship between shape and energy for clusters of adsorbed atoms (adatoms) is complicated by the significant multiatom nature (coordination dependence) of the metallic bond.[1] Multiatom interactions are responsible for much of the physics unique to metallic surfaces.[2] In particular, it has been argued that multiatom interactions play a decisive role in determining the equilibrium shapes of 2D homoepitaxial clusters of adatoms on the (111) surfaces of Cu (Ref. 4) and Pt.[5] Understanding the energetics of adatom clusters is a problem of considerable current interest in surface science. We propose to analyze this problem using a simple yet realistic model which allows the treatment of multiatom interactions. While, ideally, first-principles calculations[6] could be used to study surface cluster energetics, despite recent progress,[7–9] this still poses a formidable computational challenge. This is one reason why simplified models like the one used here are valuable. More importantly, the understanding provided by first-principles calculations is greatly enhanced when they provide the parameters for simplified models which facilitate large scale simulations and more readily provide unifying concepts.

Lattice gas models provide perhaps the most transparent framework for studying surface physics. Close-packed surfaces, such as Pt(111), are particularly well suited to investigation via lattice gas methods because, on these surfaces, adsorbate-induced relaxations are small. On more open surfaces [such as Pt(100)] the physics is complicated by larger surface relaxations.[10] Despite this apparent simplicity, the Pt(111) surface has been the focus of many recent experimental studies.[11] Because, in general, the systematic treatment of multiatom (multisite) interactions is a difficult task,[12] most lattice gas simulations of metallic surfaces to date have assumed strictly two-body (pairwise additive) interactions between atoms.[13] Because the metallic bond is strongly multiatom in nature, the situation calls for a lattice gas approach incorporating multisite interactions.

The focus of this paper is the so-called ''bond saturation model'' (BSM) and its implications for the energetics of two-dimensional homoepitaxial clusters on close-packed metallic surfaces. In Sec. II we describe the BSM, explaining how we treat interadatom bonding with three parameters (three-parameter BSM) in Sec. II A and critically discussing the resulting description of metallic bonding in Sec. II B. In Sec. II C we generalize the treatment from just interadatom bonding to all the bonds in a solid (ten-parameter BSM). In Sec. III we discuss the energetics of small clusters from the point of view of both the three-parameter (III A) and ten-parameter (III B) models and do the same for large cluster (island) energetics in Sec. IV, focusing mainly on step energies. Finally, in Sec. V, we summarize our findings and conclude.

II. BOND SATURATION MODEL

We recently proposed the ''bond saturation model'' or BSM to treat the energetics of adatoms on close-packed metallic surfaces.[14] The distinguishing feature of our approach is the inclusion of multiatom interactions in a natural and computationally convenient fashion. In the BSM, the atoms in a solid interact via *coordination dependent* nearest-neighbor bonds, i.e., the strength of the bond between two neighboring atoms depends on how many (nearest) neighbors each has. Generally, one expresses the bond strengths in terms of several bond parameters—one for each possible value of the coordination. These parameters can then be fit to *any* available (theoretical or experimental) data for the system of interest. The BSM allows one to study the consequences of coordination dependent bonding in the absence of all other physical effects, and so, to decide whether or not this effect alone can explain any given experimental finding.

A. Three-parameter BSM

An atom located on the (111) surface of an fcc crystal can occupy either an fcc or an hcp site (threefold coordinated
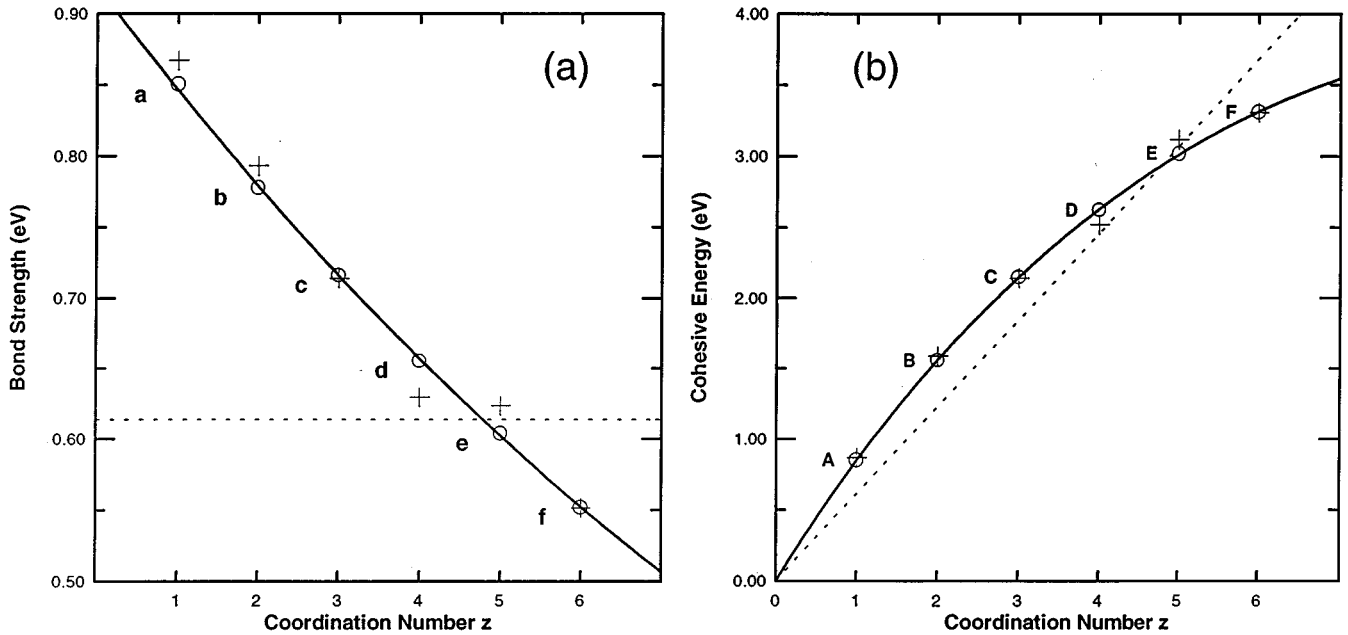
FIG. 1. Pt bond parameters [(a)] and cohesive energies [(b)] for the six-parameter BSM versus nearest adatom coordination, z. (a) is obtained by dividing all quantities in (b) by z. The parameters marked by $+$'s are determined from EAM binding energies of six clusters, whereas those marked by circles were fit to 62 binding energies. Both the solid curve (cubic polynomial) and the dotted line were fit to the refined parameters (circles) in (b).

hollow). The two types of surface sites form two (triangular) sublattices. In general, there can be interactions between adatoms on the same sublattice (at all distances, with possibly different strengths for the fcc and hcp sublattices), and also between adatoms on different sublattices. Furthermore, each of these interactions can in principle be coordination dependent. In this work, we will focus on just the nearest-neighbor bonds between adatoms on the same sublattice. This approximation is critiqued in Sec. II B.

Accordingly, for the BSM, we seek six bond parameters because each adatom can have up to six nearest (adatom) neighbors. With this scheme, the 2D lattice gas of adatoms on either sublattice is governed by a Hamiltonian of the form

$$H = -\frac{1}{2} \sum_i u(z_i) z_i n_i, \tag{1}$$

where n_i and z_i are, respectively, the occupation (1 if occupied, 0 if not) and coordination numbers at site i and $u(z_i)$ is the coordination dependent bond strength. As in Ref. 14, we obtained preliminary values for the six bond parameters [marked by $+$'s in Fig. 1(a)] from the binding energies of six clusters calculated with the embedded atom method or EAM.[15] The chosen clusters ranged in size from a dimer to a complete monolayer. From the figure, it is seen that the resulting bond strength decreases with increasing coordination as is characteristic of the metallic bond.[16] The labeling scheme in Fig. 1(a) is $u(1)=a$, $u(2)=b$, $u(3)=c$, etc. The corresponding ''cohesive energies,'' $U(z) \equiv zu(z)$, are marked by $+$'s in Fig. 1(b) and are labeled with the corresponding uppercase letters. ''Cohesive energy'' seems appropriate since in the BSM the contribution to the total energy of a solid from an atom with coordination z is proportional to $U(z)$. The cohesive energies marked by circles in Fig. 1(a) are obtained from a least-squares fit to the

EAM binding energies of 62 clusters including a monolayer and 61 clusters with up to 7 adatoms. These cohesive energies are also given in Table I. The previous energies [$+$'s in Fig. 1(b)] were used as starting values for the fit. The corresponding bond parameters [$U(z)/z$] are marked by circles in Fig. 1(a). The details for our EAM calculations and how we parametrize the binding energies are given in Ref. 14. In all our EAM calculations we used the empirical Pt function developed by Voter and Chen (VC).[17] Because the cluster binding energies calculated on the fcc and hcp sublattices differed by so little (typically several meV),[18] we averaged the two binding energies for the fit.[19]

As is seen in Fig. 1(b), the fitted cohesive energies are well described by the solid curve which is a cubic polyno-

TABLE I. Cohesive energies (least-squares fit) for Pt and coordination numbers in the six- and ten-parameter bond saturation models.

Coordination number	Parameter name	Cohesive energy (eV)	Parameter name	Cohesive energy (eV)
1	A	0.850		
2	B	1.556		
3	C	2.148	A	6.820
4	D	2.621	B	7.744
5	E	3.019	C	8.502
6	F	3.311	D	9.148
7			E	9.675
8			F	10.128
9			G	10.471
10			H	10.941
11			I	11.278
12			J	11.540

mial of the form, $U(z) = C_1 z + C_2 z^2 + C_3 z^3$ [note that we must have $U(0) = 0$]. A least-squares fit to the cohesive energies (circles) gives $C_1 = +0.9183$, $C_2 = -0.07407$, and $C_3 = +0.0022$ (eV), for the three coefficients. With this form for $U(z)$, the coordination dependent bond strength is given by

$$u(z) = C_1 + C_2 z + C_3 z^2, \qquad (2)$$

which is shown as the solid line in Fig. 1(a). Thus instead of a six-parameter model, we are behooved to think now in terms of a three-parameter model where the three coefficients (C_1, C_2, C_3) are interpreted as phenomenological constants whose values will depend on the particular system being studied. This scheme (three-parameter BSM) is quite accurate: the quadratic $u(z)$ faithfully reproduces the 62 EAM binding energies, incurring (maximum and mean) errors of only (3.4% and 0.62%).[20] In comparison, the single (coordination independent) bond strength, $u_0 \cong 0.614$ eV, obtained by fitting a straight line (dotted line with zero intercept) to the cohesive energies (circles) in Fig. 1(b), gives (max. and mean) errors of (29.2% and 18.2%). This bond [indicated by the dotted horizontal line in Fig. 1(a)] underpredicts the dimer bond strength [$u(1) \cong 0.87$ eV] by 29% and overpredicts the (saturated) monolayer bond strength [$u(6) \cong 0.55$ eV] by 11%.[21] These inaccuracies could adversely affect simulations of metal surface physics using a single coordination independent bond strength (constant bond model or CBM).

B. Critical discussion

As we have shown, the energetics predicted by EAM calculations for Pt are described very accurately in terms of (coordination dependent) nearest-neighbor bonds only. In their first-principles assessment of ''glue'' schemes (of which the BSM and EAM are examples), Robertson *et al.* found that the cohesive energies of a wide range of structures of Al atoms were determined to a large extent simply by the number of nearest neighbors, lending credence to our approach for systems other than Pt.[22] However, they found that a cohesive energy of the form $U(z) = A\sqrt{z} + Bz$ fit the first-principles energies of 18 different structures with a rather high rms deviation of 0.2 eV/atom. It is hoped that Eq. (2) better captures the essential physics for Pt and chemically similar systems, i.e., the late transition and noble metals.

With the quadratic form for $u(z)$, the BSM Hamiltonian [Eq. (1)] can be shown[14] to contain repulsive three-body (trio) and attractive four-body (quartet) interactions in addition to an attractive two-body interaction. All the trio (and separately the quartet) interactions have the same strength independent of the angles between the bonds. Though angular bonding is precluded in the EAM through the assumption of rigid spherical atomic charge densities, substrate relaxations can, in principle, induce effectively angle-dependent interactions. But by the close agreement between the BSM and the EAM, we infer that the EAM predicts small surface relaxations—as expected for close-packed surfaces. Because of this explicit lack of angular dependence, the BSM is probably not well suited, in its present form, to more open surfaces which can have significant surface relaxations[10] and

also, as emphasized by Einstein,[23] to the central transition metals where angular bonding is important.[24]

The energetics embodied by Eqs. (1) and (2) work quite well (at least at the EAM level) when all the adatoms reside on the same sublattice. The most serious omission is probably the (next longest) bond between adatoms on the two different sublattices (i.e., between an atom on an fcc site and one on a nearby hcp site). However, our EAM calculations indicate that this ''mixed-site'' bond is on average about 0.1 eV weaker than the ''pure-site'' bond (0.7 eV average).[14] Also, most of the mixed-site clusters we studied relaxed (at $T=0$) into homogeneous-site clusters. This is perhaps a further indication of the tendency for adatoms to occupy the same type of surface site. A recent study by Feibelman, Nelson, and Kellogg[9] is also of significance here. Using field-ion microscopy (FIM), they observed that a single Pt adatom on Pt(111) prefers to bind at fcc sites. This observation is corroborated by their first-principles calculations which indicate a preference of 0.18 eV for adatom binding at an fcc site over an hcp site (the EAM predicts a negligible difference of ~1 meV). The formation of mixed-site bonds would then be hindered because adatoms would tend to avoid the hcp sites.

C. Ten-parameter BSM

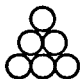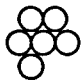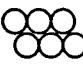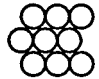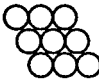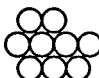We have extended our approach to treat all the (nearest-neighbor) bonds in a solid instead of just interadatom bonds as discussed so far. Our motivation is simple: with the model discussed in the preceding section, we can only 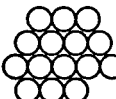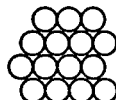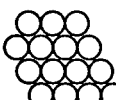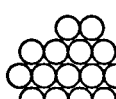study two-dimensional surfaces. Extending the model to all bonds allows us to study three-dimensional surface physics. In this work, we will use this extended model to examine the influence of substrate atom coordination on 2-D cluster energetics.

Since an adatom on an fcc (111) surface always has three nearest neighbors in the substrate and can have 0 to 6 adatom neighbors, its coordination (now total number of nearest neighbors) can have any value from 3 to 9. The coordination of substrate atoms can vary from 9 (no adatom neighbors) to 12 (bulk coordinated). Accordingly, we seek 10 bond parameters to characterize bonding over the entire range of coordination numbers from 3 to 12. The Hamiltonian for this ten-parameter BSM will also be given by Eq. (1) but with a possibly different form for $u(z)$ (and a different range for z). The contribution to the energy of a solid from an atom with coordination z will again be $-U(z)/2$ [recall $U(z) \equiv zu(z)$]. In keeping with the previous labeling scheme, we have

$$J \equiv U(12), \quad I \equiv U(11), \quad H \equiv U(10), \dots, \quad A \equiv U(3). \qquad (3)$$

We could not find ten (2D) clusters which would give ten *independent* equations in the ten unknown bond parameters.[25] Rather, we obtained the ''bulk energies,'' H, I, and J from three bulk quantities for Pt: the measured sublimation (E_{sub}) and vacancy formation (E_v^f) energies and a calculated value for the divacancy removal energy (E_{2v}^r). In the BSM, $E_{sub} = J/2$, since it is the energy (per atom) required to break up an infinite solid into isolated atoms. E_v^f is the energy cost *beyond* E_{sub} to remove a single atom from the bulk. Removing this atom changes the coordination numbers of its 12 nearest neighbors from 12 to 11. Thus, $E_v^f = 6(J - I)$. Similar reasoning gives $E_{2v}^r = 10J - 7I - 2H$, which is the energy to remove two neighboring atoms from

M. C. FALLIS AND C. Y. FONG

TABLE II. EAM and BSM (three and ten parameter) binding energies (eV) and 0th–3rd coordination moments for clusters in three bond maximizing groups.

CLUSTER	EAM	3p BSM	10p BSM	m_0	m_1	m_2	m_3
	6.241 6.284	6.278	6.236 6.294	6	18	60	216
	6.299	6.284	6.288	6	18	60	222
	6.332	6.332	6.325	6	18	58	198
	10.556	10.568	10.560	9	32	128	566
	10.585	10.616	10.597	9	32	126	542
	10.576 10.595	10.616	10.568 10.626	9	32	126	542
	10.627	10.623	10.620	9	32	126	548
	19.502 19.510	19.533	19.497 19.526	15	62	282	1388
	19.504 19.511	19.533	19.497 19.526	15	62	282	1388
	19.530 19.538	19.581	19.534 19.563	15	62	280	1364
	19.572 19.557	19.588	19.557 19.586	15	62	280	1370

the bulk. Foiles, Baskes, and Daw (FBD) report measured values from the literature of 5.77 and 1.5 eV for E_{sub} and E_v^f for Pt.[26] These give 11.54 and 11.29 (eV) for J and I, respectively. E_{2v}^r is not directly measurable and the measured values reported by FBD for the related divacancy binding energy (E_{2v}^b) are quite uncertain: 0.1–0.2 eV. Using the VC EAM Pt function, we obtained 14.472 eV for E_{2v}^r (unrelaxed), giving 10.95 eV for H.[27] As a consistency check, we
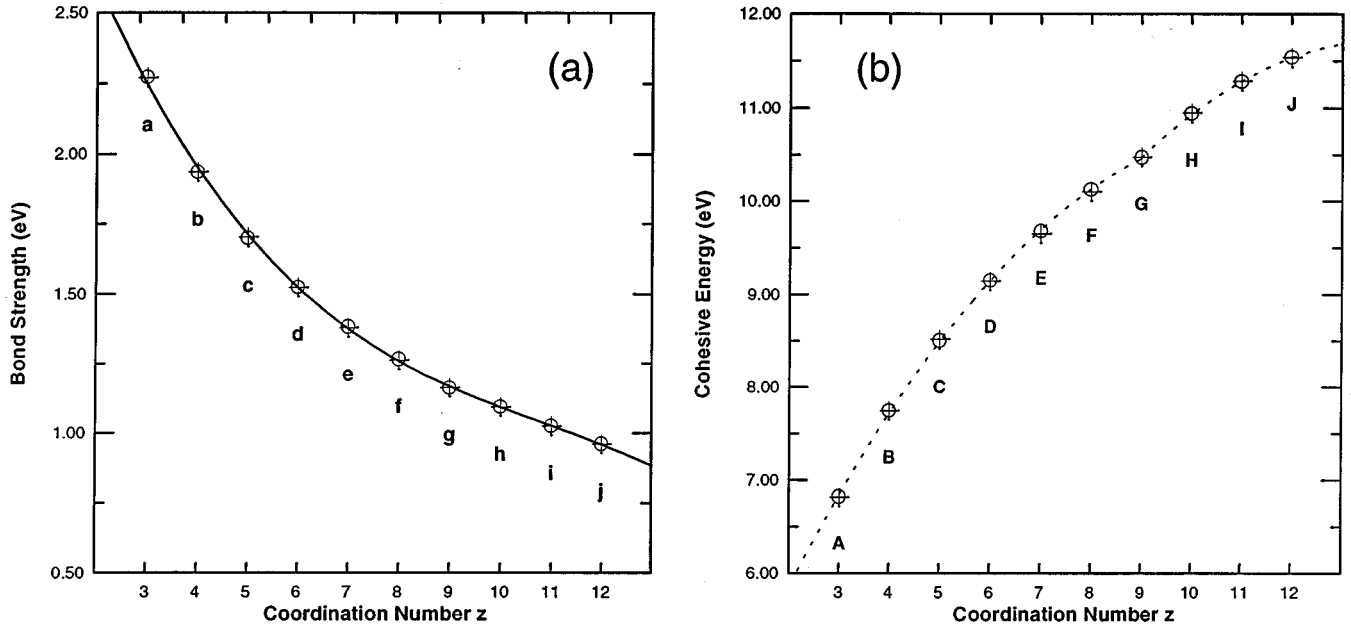
FIG. 2. Pt bond parameters [(a)] and cohesive energies [(b)] for the ten-parameter BSM versus *total* nearest-neighbor coordination, z. All symbols have the same meaning as in Fig. 1. The solid curve in (a) is a fourth degree polynomial fit to the parameters (circles) in (b) [not shown in (b) for clarity]. The dotted curve in (b) is meant only as a guide to the eye.

note that with H, I, and J determined as described, the model value for the divacancy binding energy, $E_{2v}^b \equiv |E_{2v}^r - 2(E_{sub} + E_v^f)| = 3J - 5I + 2H$, is about 0.07 eV (attractive). This is much closer to the experimental range than 0.45 eV, obtained with the FBD EAM Pt function.[26] This attests to the accuracy of both the VC Pt potential as well as the description of bonding provided by the (ten-parameter) BSM.

With the bulk energies $(H-J)$ determined, we then picked seven clusters from the 62 in Ref. 14 and solved the resulting seven equations in the seven unknown ''adatom energies,'' $A-G$.[28] As in Fig. 1, these preliminary energies are marked by $+$'s in Fig. 2(b) as are the corresponding bond parameters in Fig. 2(a). As before, these parameters were used as starting values for a least-squares fit to the EAM binding energies of the same 62 clusters giving the parameters marked by circles in Figs. 2(a) and 2(b). The parameters changed much less for the ten-parameter fit (maximum of 0.25% for E) than for the six-parameter fit (4% for D). The dotted line in Fig. 2(b) is meant only as a guide to the eye but it does indicate that the ten energies are best fit by two functions which meet at G where there is a cusp in both parameter sets. The solid curve in Fig. 2(a) is a third degree polynomial of the form, $C_1 + C_2 z + C_3 z^2 + C_4 z^3$ fit to the circles in Fig. 2(b) (not shown there for clarity). The fitted coefficients are $C_1 = +3.563\,47$, $C_2 = -0.561\,972$, $C_3 = +0.045\,241$, and $C_4 = -0.001\,373\,92$. This shows that we really need only four parameters instead of ten. For this work, we choose to work directly with the ten (least-squares) parameters which are listed in Table I. Unless stated otherwise, any numerical result we give for the ten-parameter BSM is obtained with these values. The ten-parameter BSM is not only more accurate than the three-parameter model, but, as we shall see, also gives qualitatively different physics in the sense that it predicts different values for physical quantities which are degenerate in the three- (or six-) param-

eter model. It should be stressed that there is nothing sacred about fitting the BSM parameters to EAM calculations and that in general any theoretical (e.g., first-principles calculations) or, better yet, experimental data could be used.

III. SMALL CLUSTER ENERGETICS

A. Energy-shape relationship in the three-parameter BSM

To demonstrate the predictive power of our method, let us switch in Eq. (1) from a summation over lattice sites to a summation over coordination numbers, giving

$$H = -\frac{1}{2} \sum_{z=0}^{6} z u(z) N_z, \qquad (4)$$

where N_z is the coordination distribution giving (for each z) the number of adatoms with that coordination. Using the quadratic form for $u(z)$ in Eq. (2), Eq. (4) becomes

$$H = -\frac{1}{2} [C_1 m_1 + C_2 m_2 + C_3 m_3], \qquad (5)$$

where m_1, m_2, m_3 are the first, second, and third moments of N_z—the pth moment being defined as, $m_p \equiv \sum_{z=0}^{6} z^p N_z$. In the remainder of this section, we will explore the ramifications of this ''moment expansion'' of the BSM Hamiltonian for the energetics of $2D$ adatom clusters.

Since in any (finite) cluster there must be some adatoms with $z<6$, we have, $6m_p > m_{p+1}$, and for our parameters, $C_1 > 6|C_2| > 36C_3$. These two facts are sufficient to establish $C_1 m_1 > |C_2| m_2 > C_3 m_3$, and therefore, $C_1 m_1 > |C_2 m_2 + C_3 m_3|$, because C_2 and C_3 have opposite signs. Thus, because C_1 is attractive (positive), the energy of a cluster of N (m_0) adatoms is minimized by *first* maximizing m_1 which is just twice the number of (nearest-neighbor) bonds. So far, we have not made any pre-

dictions different from a constant bond model. For $N=2,3,4,5,7,8,10,12,14,16,19$, etc., there is *only one* bond-maximizing cluster geometry. However, when there are several different bond-maximizing geometries (as for $N=6,9,11,13,15,17,18$, etc.), the higher moment terms in Eq. (5), *which are absent in a constant bond model*, determine which shapes are most stable. Because the second moment term (next largest) is *repulsive*, for fixed m_0 and m_1 the most highly bound clusters will *minimize m_2*. Thus, since m_2 is a measure[29] of the width of the coordination distribution, it is energetically favorable to have the ''populated'' values of z gathered as closely as possible around the mean value: $\bar{z}=m_1/m_0$. Lastly, for cluster geometries with the same m_0, m_1, and m_2, it is energetically favorable to maximize m_3 which is a measure[29] of the asymmetry of N_z.

The above scheme is nicely illustrated in Table II for the bond-maximizing geometries with 6, 9, and 15 adatoms. For each cluster, we list the binding energies calculated (on the fcc sublattice) with the EAM (Ref. 14) and with the three- and ten-parameter forms of the BSM in columns 2–4, and the 0th–3rd moments of N_z in columns 5–8. The three cluster shapes in the upper group all have 6 (m_0) adatoms and 9 ($m_1/2$) bonds. As expected, the geometry with the smallest value of m_2 has the highest binding energy (in all three models). In the three-parameter BSM, the binding energies of the other two geometries (with equal m_2) increase with the value of m_3. The same remarks hold true for the 9 and 15 adatom groups as well. Because the BSM can so accurately reproduce the EAM results, we believe the conclusions drawn here for Pt(111) should also hold for the (111) surfaces of the other ''EAM metals'': Ni, Cu, Pd, Ag, and Au.

This relatively simple scheme is complicated by the fact that some clusters' binding energies depend on how they are oriented on the (111) surface.[3,14,30] Clusters of this type have two binding energies listed in columns 2 and 4 (EAM and ten-parameter BSM). The two binding energies correspond to two orientations which differ by a 180° rotation of the entire cluster. As we show in the next section, this difference can be understood in the context of the ten-parameter BSM. Keeping this complication in mind, we assert that the rule of thumb: ''first maximize m_1, then minimize m_2, and finally maximize m_3,'' should provide a unique and powerful way of deciphering the spectrum of binding energies of 2D homoepitaxial adatom clusters on close-packed surfaces of the EAM metals. This hypothesis should be testable (although not without care as evidenced by the small energy differences in Table II) by observing adatom clustering with FIM or similar techniques for probing surfaces. To our knowledge, the only fcc (111) surface on which many small homoepitaxial clusters have been studied in atomic detail is Ir(111) by Wang and Ehrlich.[30] Using FIM, they observed clusters with 2–8, 12, and 13 adatoms. With the exception of trimers, they always observed bond-maximizing equilibrium geometries in agreement with our hypothesis. However, for clusters with 6 and 13 adatoms (for which there are several possible bond-maximizing geometries), they observed different ground state geometries than predicted by our rule. These ''discrepancies'' probably just reflect the increased angular character of the Ir bond compared to the Pt bond.[24]
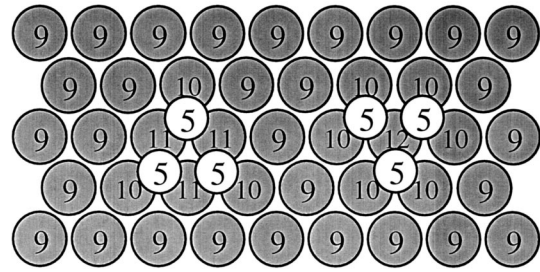

FIG. 3. The two physically distinct orientations of a compact trimer on a fcc (111) substrate. The ''hollow'' configuration is on the left and the ''filled'' configuration on the right. If the $[\bar{1}\,\bar{1}2]$ direction is up, then the adatoms (smaller open circles) reside on fcc sites. Only the top layer substrate atoms (shaded circles) are shown. All atoms in the figure are labeled with their total nearest-neighbor coordination (z in the ten-parameter BSM).

B. Effect of cluster orientation on binding energy

As mentioned in the preceding section, the binding energies of certain clusters depend on how they are oriented on the substrate. The two possible orientations of a triangular trimer on the fcc sublattice[31] are shown in Fig. 3. The triangle on the left (pointing up) is centered on a surface hollow (hcp site), while the triangle on the right (pointing down) is centered on a substrate atom. Following Ref. 14, we will refer to these as ''hollow'' and ''filled'' orientations, respectively. According to our EAM calculations, the filled trimer is more stable than the hollow trimer by about 40 meV. This may not seem surprising given that the adatoms bond to seven substrate atoms in the filled trimer, but to only six in the hollow trimer as is clear from Fig. 3. However, it should be noted that the number of bonds is the same for both configurations. This is easily seen by summing the coordination numbers (which overcounts bonds by a factor of 2) of the seven substrate atoms for the filled trimer: $6(10)+12=72$, and doing the same for the hollow one: $9+3(10)+3(11)=72$ (a seventh substrate atom contributes the 9). Clearly, the coordination numbers of the adatoms and the rest of the substrate atoms cancel in the energy difference between the two trimers. Thus, from the vantage of (nearest-neighbor) lattice gas models, this difference is a purely multiatom effect not understandable in a constant bond model (CBM). Rotating the trimer does not affect the number of bonds, but it does affect their strengths. This is reflected in the ten-parameter expression for the energy difference,

$$\Delta E_{fh}=-\frac{1}{2}\left[(J-G)-3(I-H)\right], \qquad (6)$$

where ΔE_{fh} stands for $E_{\text{filled}}-E_{\text{hollow}}$. Note that ΔE_{fh} reduces to zero in a CBM where $U(z)=zu_0$ [refer to Eq. (3)]. The BSM value of about -29 meV for this quantity reflects the higher stability of the filled trimer. The (average) EAM value for this quantity obtained from all the ''polar'' clusters (see the next paragraph) in the set of 62 is -28.6 meV. Note that, for $T<250$ K, Wang and Ehrlich observed triangular Ir trimers in the hollow configuration 80% of the time[30] in contrast to our prediction for enhanced stability of the filled trimer.

Since larger clusters are composed of both hollow and filled triangles, any cluster with an excess of either kind of triangle is expected to have a preferred orientation. It is just these ''polar'' clusters which have two binding energies in Table II for the EAM and ten-parameter BSM. If the page of the figure is the (111) substrate with the [1 1̄ 2] direction pointing up and the [1̄10] direction to the right (as in Fig. 3), the upper binding energy corresponds to the (hollow) orientation (shown in column 1), and the lower value to the rotated (filled) orientation (not shown). Except for the bottommost 15-adatom cluster, both the EAM and the ten-parameter BSM predict that the filled orientation is most stable. As is shown in Sec. IV B, in the ten-parameter BSM, the energy difference between the two orientations is always a multiple of the fundamental difference, ΔE_{fh}, in Eq. (6). This need not be true in the EAM because the forces are of longer range and there is surface relaxation. The two orientations are degenerate in the three-parameter BSM, because coordination changes for atoms in the substrate are ignored, whereas, in the EAM and ten-parameter BSM, they are included and give rise to an energy difference.

IV. LARGE CLUSTER (ISLAND) ENERGETICS

A. Binding energy in the three-parameter BSM

To further clarify the energy-shape relationship, we calculate the binding energy according to Eq. (4) of an arbitrary cluster assuming only that, for every adatom, $z \geq 2$. An N-adatom cluster (like any of those in Table II) will have L adatoms (with $z < 6$) on the perimeter, and $N-L$ (interior) adatoms with $z = 6$, where L is the perimeter length in units of the lattice constant. The L perimeter adatoms can be divided into N_c corner adatoms and $L-N_c$ edge adatoms with $z = 4$. The N_c corner adatoms can be divided into N_2, N_3, and N_5 adatoms (with z's of 2, 3, and 5). Since, by assumption, $N_0 = N_1 = 0$, we now have the entire coordination distribution. Replacing $-zu(z)/2$ in Eq. (4) by U_z, the cluster's binding energy, E_{bind}, is then given by

$$E_{\text{bind}} = U_6 N + U_{46} L + U_{24} N_2 + U_{34} N_3 + U_{54} N_5, \quad (7)$$

where $U_{nm} \equiv U_n - U_m$ is the energy cost of changing the coordination of an adatom from m to n. The physical interpretation of the terms in this expression is obvious: $U_6 N$ is the ''bulk'' or ''interior'' energy, $U_{46} L$ is the energy cost of creating the cluster boundary (step energy), and the next three terms are the energy costs of putting bends with angles (measured inside the cluster) of 60°, 120°, and 240° in the boundary (corner energies). In terms of C_1, C_2, and C_3, these energies are $U_6 = -3C_1 - 18C_2 - 108C_3 \cong -1.66$, $U_{46} = C_1 + 10C_2 + 76C_3 \cong +0.34$, $U_{24} = C_1 + 6C_2 + 28C_3 \cong +0.53$, $U_{34} = (C_1 + 7C_2 + 37C_3)/2 \cong +0.24$, and $U_{54} = -(C_1 + 9C_2 + 61C_3)/2 \cong -0.19$ (all in eV/adatom). In contrast, for a CBM we have (in the same order): -1.84, $+0.61$, $+0.61$, $+0.31$, -0.31 (eV/adatom), using the single bond, $u_0 = 0.614$ eV (Sec. IIA), in place of C_1 and taking $C_2 = C_3 = 0$. The ratios of the BSM to the CBM values for these quantities are: 0.90, 0.56, 0.87, 0.77, and 0.61, respectively. Their magnitudes, especially the step energy (U_{46}), are reduced in the BSM by the repulsive nature of C_2 (i.e., by repulsive three-body interactions[14]). Consequently, we should expect the BSM lattice gas to disorder at lower temperatures than the corresponding CBM. For example, island edges should roughen at lower temperatures in the BSM than in the CBM. Our Monte Carlo simulations do indeed show this and other interesting phenomena.[32] Note that Eq. (7) could be useful in determining C_1, C_2, and C_3 directly from experiment.

B. Step energies and island shapes

The above value, $U_{46} \cong 343$ meV/adatom for the step energy, agrees well with the EAM calculations of Nelson et al.[33] (NEKR), who obtained ($T = 0$) step energies of (359 and 357 meV/adatom) with the VC Pt potential, and (344 and 341 meV/adatom) with the FBD potential for (A and B) type steps on Pt(111). The A ({100} microfacet) and B ({111} microfacet) step energies are degenerate in the three- (or six-) parameter BSM and, as we shall see, are nearly so in the ten-parameter model.

Arguing plausibly that maximizing the number of bonds is equivalent to maximizing N_6, since $L = N - N_6$, it follows that the ground state shapes predicted by Eq. (7) will have minimum perimeter length L. This is equivalent to saying that the boundary energy term ($U_{46} L$) is the dominant edge term in Eq. (7). This is clearly the case for a large island with long straight edges because edge atoms will far outnumber corner atoms. Attempting to lower the energy by forming five fold coordinated corners ($U_{54} < 0$) would not seem to balance the cost of increasing L. This reasoning appears to hold even for *small* clusters since, in Table II, all the clusters in a given group have the same L. To minimize L, large clusters will tend to form hexagons with sides of equal length.[34] Thus, for Pt, *despite the multisite interactions* in the three-parameter BSM, the predicted ground state cluster shapes are regular hexagons.

In the STM experiments of Michely and Comsa,[5] for $T > 700$ K, hexagonal clusters on the Pt(111) surface are indeed seen but with sides that alternate in length in an $ABABAB$ fashion with A steps short and B steps long. They observe the same shapes independent of the islands' sizes and independent of their formation history and thus conclude that these represent *equilibrium* island shapes. The measured ratio of the short to long side lengths, 0.66 ± 0.05, gives via the Wulff construction[35] a free energy ratio, $R \equiv f_B / f_A = 0.87 \pm 0.02$, for the two steps. That is, on Pt(111), B steps have *lower* free energy than A steps. Michely and Comsa (MC) remark that it is natural to expect the {111} microfacet (B step) to have a lower energy because the (111) surface (with its higher coordination) is lower in energy than any other surface. This very plausible sounding argument is actually misleading. First of all, for a *monatomic* step, the concept of a microfacet is not really valid since none of the atoms at the step (on the upper or lower terrace) have the same coordination as for the true facet. Still, the B step, for which the atoms at the step bottom have 11 nearest neighbors, is more highly coordinated than the A step for which the corresponding coordination number is 10 (see Fig. 4). This would seem to lend credence to MC's reasoning. Indeed, as we will show, if the A and B steps differed *only* in the coordination of the step atoms, the B step would have a substantially lower (ground state) energy than the A step in agreement with MC. However, it is crucial to note that the two steps differ also in their ''unit cell'' areas (Fig. 4). As we
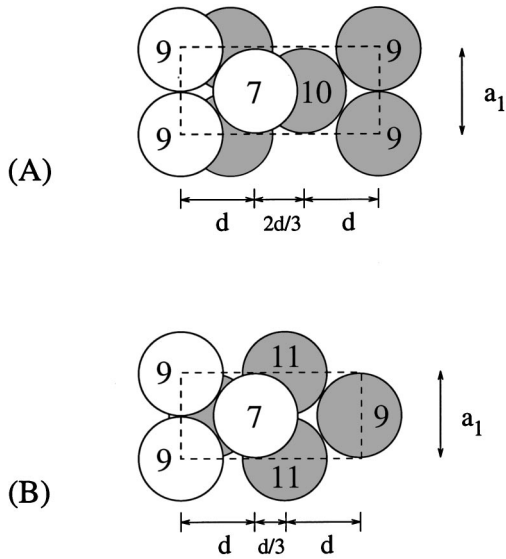
FIG. 4. Unit cells (inside dashed boundary) for the A ({100} microfacet) (upper figure) and B ({111} microfacet) (lower figure) steps on a fcc (111) surface. Repeating the cells vertically will create steps running vertically. As in Fig. 3, the atoms are labeled with their nearest-neighbor coordination. Unshaded atoms reside in the upper terrace and shaded atoms in the lower terrace. In the figure, a_1 is the nearest-neighbor bond length, in terms of which $d = \sqrt{3}a_1/2$. Thus the two cells differ in length by only $a_1/2\sqrt{3}$.

shall see, this areal difference translates into a substantial energy difference and results in essentially degenerate step energies in disagreement with MC's remark and with the observed step (free) energy difference.

To calculate a step energy, one could proceed in the following manner. First calculate the surface energy of a substrate which is slightly miscut and so has a surface with wide terraces bounded by parallel monatomic steps. This surface energy will include both step and terrace energies (and presumably minimal step-step interactions for sufficiently wide terraces). To obtain the step energy, one subtracts the proper amount of terrace energy.[36] The essence of this calculation is a subtraction of surface energies in the immediate vicinity of the step.[37] Accordingly, we take,

$$\beta_{\text{step}} = [\epsilon_{\text{step}} - \epsilon_{\text{terrace}}] A_{\text{step}} / a_{\parallel}, \qquad (8)$$

as our definition of step energy. Here β_{step} is the step energy/atom (or per unit step length), ϵ_{step} and $\epsilon_{\text{terrace}}$ are the step and terrace surface energies per unit area, A_{step} is the area of the step unit cell, and $a_{\parallel}$ is the width of the step unit cell parallel to the step (i.e., the spacing between neighboring atoms along the step).

In Eq. (8), $\epsilon_{\text{step}} A_{\text{step}}$ is just the surface energy of the step unit cell. The unit cells for monatomic A and B steps on the (111) surface are depicted in Fig. 4. Each surface atom contributes, $U_z - U_{12}$ to the surface energy where U_z has the same meaning as in Eq. (7) and z is the atom's surface coordination. Thus, the unit cell energies for A and B steps are $\epsilon_A = U_7 + U_9 + U_{10} - 3U_{12}$ and $\epsilon_B = U_7 + U_9 + U_{11} - 3U_{12}$, respectively. In terms of the cohesive energies $A - J$ we have $\epsilon_A = [3J - (H + G + E)]/2$ and $\epsilon_B = [3J - (I + G + E)]/2$. The difference in cell energies, $\epsilon_A - \epsilon_B = (I - H)/2 \cong 0.17$ eV/atom, is purely due to the different coordination of the atoms

at the bottom of the two steps. If this were the only difference between the two step energies, B steps would be substantially favored. According to Eq. (8) we must subtract from the unit cell energy, $\epsilon_{\text{terrace}} A_{\text{step}}/a_{\parallel}$, which for the problem at hand becomes $\epsilon_{111} l_{\text{step}}$, where ϵ_{111} is the (111) surface energy per unit area and l_{step} is the step unit cell length (perpendicular to the step). By the previous discussion, we have $\epsilon_{111} = (J - G)/2 \cong 535$ meV/atom. In terms of the nearest-neighbor bond length a_1, the surface area per atom on the (111) surface is $\sqrt{3}a_1^2/2$, giving $\epsilon_{111} = (J - G)/\sqrt{3}$ eV/a_1^2, or about 1288 erg/cm^2 for the Pt(111) surface energy. Full scale EAM calculations give 1341 erg/cm^2 (VC) (Ref. 38) and 1440 erg/cm^2 (FBD).[26,39] The lack of surface relaxations in the BSM can always be invoked as the culprit behind any discrepancy with the EAM. From Fig. 4, the A and B step unit cell lengths are seen to be $l_A = 4a_1/\sqrt{3}$ and $l_B = 7a_1/2\sqrt{3}$. Thus the terrace subtraction term is $4(J - G)/3$ for A steps and $7(J - G)/6$ for B steps (both eV/atom). Combining everything, we have

$$\beta_A = \frac{1}{2}[3J - (H + G + E)] - \frac{4}{3}(J - G), \qquad (9)$$

and

$$\beta_B = \frac{1}{2}[3J - (I + G + E)] - \frac{7}{6}(J - G) \qquad (10)$$

for the A and B step energies in the BSM. These expressions give $\beta_A = 341$ meV/atom and $\beta_B = 351$ meV/atom, in good agreement with NEKR's EAM results. While NEKR found a very slight preference (2–3 meV) for the B step, we predict a slight preference (10 meV/atom) for A steps. These small energy differences are certainly near if not well below the limit of accuracy of the EAM.

The step energy difference is, from Eqs. (9) and (10),

$$\beta_A - \beta_B = \frac{I - H}{2} - \frac{J - G}{6}. \qquad (11)$$

The first term (0.169 eV/atom), as previously discussed, has its origin in the different coordination of atoms at the step bottom and strongly favors B steps. The second term (0.178 eV/atom), arising from the difference in unit cell areas, is large enough to cancel the first term and even tip the scales slightly the other way in favor of A steps. Note that the absence of substrate contributions in the three- (or six-) parameter BSM is responsible for the consequent degeneracy of the two step energies. In the limit of a single bond strength (CBM), both Eqs. (9) and (10) reduce to u_0 per atom, so that their difference (if any) is purely multiatom in origin.

For self-consistency, we now show that the step energy difference obtained above for infinitely long steps can also be obtained from the energetics of finite clusters. To do this, consider two clusters shaped like equilateral triangles, each with three sides of length S (in lattice parameter units), one (hollow, with B-type edges) pointing up and the other (filled, with A-type edges) pointing down. The $S=1$ case is shown in Fig. 3. Just as for the trimer ($S=1$) considered in Sec. III B, the binding energy difference for the two clusters will only have contributions from the substrate atoms. Accordingly, we seek the number (N_z) of substrate atoms with

z's of 10, 11, and 12. For the filled cluster, we have $N_{12}=S(S+1)/2$, $N_{11}=0$, $N_{10}=3(S+1)$, and for the hollow cluster $N_{12}=S(S-1)/2$, $N_{11}=3S$, and $N_{10}=3$. Therefore, the filled cluster bonds to S more substrate atoms than the hollow one. Being careful to treat this difference in number of substrate atoms, we find

$$E_{\text{filled}}-E_{\text{hollow}}=S\Delta E_{fh} \qquad (12)$$

for the energy difference. In accord with the discussion in Sec. III B, it is a multiple of the fundamental difference for trimers in Eq. (6). Since rotating any cluster by 180° converts its A-type edges into B and vice versa, we must conclude that ΔE_{fh} is related to the A,B step energy difference. This has been explicitly demonstrated by Barkema *et al.*,[3] who studied equilibrium island shapes on close-packed surfaces using an Ising model with two- and three-spin interactions, with the energy difference between up and down trimers (treated as a phenomenological parameter) governing the strength of the three-spin terms.[40] Their argument is simple: adatoms in a cluster's interior belong to equal numbers of up and down triangles and so do not contribute to the orientational energy difference, whereas an adatom in an A step belongs to 2 down and 1 up triangle and vice versa for B steps. It is then natural to write Eq. (12) as

$$E_{\text{filled}}-E_{\text{hollow}}=3[\Delta\beta_{\text{corner}}+(S-1)\Delta\beta_{\text{step}}],$$

where $\Delta\beta_{\text{corner}}$ and $\Delta\beta_{\text{step}}$ are the corner and step energy differences, respectively. Now when Eq. (12) is written as

$$E_{\text{filled}}-E_{\text{hollow}}=3[1+(S-1)]\Delta E_{fh}/3,$$

we see by comparison with the previous expression that

$$\Delta\beta_{\text{corner}}=\Delta\beta_{\text{step}}=\Delta E_{fh}/3.$$

From Eq. (6) we then have

$$\Delta\beta_{\text{step}}=\beta_A-\beta_B=\frac{I-H}{2}-\frac{J-G}{6},$$

in agreement with Eq. (11).

By estimating step energies from EAM surface energies corresponding to the step microfacet,[41] NEKR find, either degenerate step energies ($\beta_B/\beta_A\cong1.0$) for (Ag,Au,Pt), or a slight preference for A steps ($\beta_B/\beta_A\cong1.1$) for (Cu, Ni, Pd).[33] There is strong (if indirect) evidence from experiment that A steps are favored on Cu(111).[4] This is corroborated by Breeman *et al.*'s semiempirical (Finnis-Sinclair method) study of Cu clusters on Cu(111).[42] It therefore seems that the prediction of nearly degenerate A and B step energies is generic to atom-embedding schemes. Given Michely and Comsa's (MC) finding of lower B step free energies, we might be tempted to conclude that the Pt(111) surface is exhibiting non-EAM behavior. However, in a recent *first-principles* study of steps on Pt(111), Feibelman found higher but still essentially degenerate ground state A and B step energies: 0.46 and 0.47 eV/atom for β_A and β_B, respectively.[43] Feibelman's finding is contested by a more recent first-principles study by Boisvert *et al.*[44] Their preliminary results for the same step energies are in excellent agreement with MC. It

should be emphasized that finite temperature effects could play a significant role in the analysis of MC's discovery. After all, the ratio of step free energies reported by MC is inferred from observations of clusters equilibrated at $T>700$ K. Assuming Feibelman's result for β_A is representative of the free energy (f_A), MC's reported ratio ($f_B/f_A=0.87\pm0.02$) implies a free energy difference (f_A-f_B) of only 60 ± 10 meV/atom. The thermal energy k_BT has roughly the same value (60 meV) at $T=700$ K. NEKR have shown that entropic contributions to the step free energies from ''diffusional step wandering'' are negligible[33] but this has not been shown for the effects of vibrational entropy.

V. CONCLUSION

In conclusion, we have studied the role played by multiatom interactions in determining the energies and shapes of 2D homoepitaxial adatom clusters on close-packed metallic surfaces using the ''bond saturation model'' or BSM. By describing adatom-adatom interactions in terms of *coordination dependent* nearest-neighbor bonds only, we arrive at a very detailed understanding of the energy-shape relationship for adatom clusters predicted with EAM calculations. Key to this relationship, for the three-parameter BSM, is an expansion of the model Hamiltonian in the moments of the distribution of adatom coordination numbers. This expansion leads to a simple rule for predicting how the binding energies of several bond-maximizing cluster shapes will order. This rule should be testable with surface probes such as FIM or STM. We have also obtained a simple expression for the binding energy of a cluster of arbitrary shape which includes step and kink energies.

Hexagons (with sides of equal length) are the predicted ground state shapes for large clusters in the three-parameter BSM (as in an Ising model with a single nearest-neighbor bond strength). In contrast, on Pt(111) (for $T>700$ K), the experimentally observed island shapes are hexagons with sides that alternate in length indicating a lower free energy for B steps (111 microfacet) than A steps (100 microfacet). The two step energies are degenerate in the three- (and six-) parameter BSM's (adatom-adatom bonding only), but with the treatment of adatom-substrate bonding in the ten-parameter BSM, this degeneracy can in principle be lifted. However, the two step energies are nearly degenerate even in the ten-parameter BSM because the two factors which determine the step energies, namely, the difference in coordination of the atoms at the step bottom (favoring B steps by ~170 meV/atom) and the difference in step unit cell areas (favoring A steps by ~180 meV/atom) give nearly cancelling energies. This gives insight as to why the experimentally observed step free energy difference is small (~60 meV/atom). The BSM allows powerful conclusions to be drawn with relative ease even in the presence of multiatom interactions which, at first glance, would seem to place such analysis out of easy reach.

[1] (a) A. E. Carlsson, in *Solid State Physics*, Vol. 43, edited by H. Ehrenreich and D. Turnbull (Academic Press, San Diego, 1990); (b) J. K. Nørskov, in *The Chemical Physics of Solid Surfaces*, Vol. 6, *Coadsorption, Promoters and Poisons*, edited by D. A. King and D. P. Woodruff (Elsevier, Amsterdam, 1993).

[2] For example, the (1×2) ''missing-row'' reconstruction of Au and Pt(110) can be viewed, to first order, as the result of competition between attractive second-nearest-neighbor and repulsive *three-body* nearest-neighbor interactions: S. M. Foiles, Surf. Sci. **191**, L779 (1987).

[3] G. T. Barkema, M. E. J. Newman, and M. Breeman, Phys. Rev. B **50**, 7946 (1994).

[4] T. Klas *et al.*, Europhys. Lett. **7**, 151 (1988).

[5] T. Michely and G. Comsa, Surf. Sci. **256**, 217 (1991).

[6] M. C. Payne *et al.*, Rev. Mod. Phys. **64**, 1045 (1992).

[7] S. Oppo, V. Florentini, and M. Scheffler, Phys. Rev. Lett. **71**, 2437 (1993).

[8] R. Stumpf and M. Scheffler, Phys. Rev. Lett. **72**, 254 (1994).

[9] P. J. Feibelman, J. S. Nelson, and G. L. Kellogg, Phys. Rev. B **49**, 10 548 (1994).

[10] A. F. Wright, M. S. Daw, and C. Y. Fong, Phys. Rev. B **42**, 9409 (1990).

[11] C. Teichert *et al.*, Phys. Rev. Lett. **72**, 1682 (1994); T. Michely *et al.*, *ibid*. **70**, 3943 (1993); M. Bott *et al.*, *ibid*. **70**, 1489 (1993); G. Rosenfeld *et al.*, *ibid*. **70**, 3943 (1993); Ref. 5.

[12] T. L. Einstein, Langmuir **7**, 2520 (1991).

[13] C. Ratsch *et al.*, Surf. Sci. **329**, L599 (1995); J. G. Amar and F. Family, Phys. Rev. Lett. **74**, 2066 (1995); G. S. Bales and D. C. Chrzan, Phys. Rev. B **50**, 6057 (1994); N. C. Bartelt, T. L. Einstein, and E. D. Williams, Surf. Sci. **312**, 411 (1994); M. Baba, A. Natori, and H. Yasunaga, *ibid*. **239**, 363 (1990).

[14] M. C. Fallis, M. S. Daw, and C. Y. Fong, Phys. Rev. B **51**, 7817 (1995).

[15] A comprehensive review: M. S. Daw, S. M. Foiles, and M. I. Baskes, Mater. Sci. Rep. **9**, 251 (1993).

[16] Ref. 1(a), pp. 29 and 30, and 1(b), pp. 14–18.

[17] A. F. Voter, Los Alamos National Laboratory Technical Report No. LA-UR-93-3901, 1993; A. F. Voter and S. P. Chen, in *Characterization of Defects in Materials*, edited by R. W. Siegel, J. R. Weertman, and R. Sinclair, MRS Symposium Proceedings No. 82 (Materials Research Society, Pittsburgh, 1987), p. 175.

[18] Thus, the EAM predicts the same nearest-neighbor interactions on both fcc and hcp sublattices. It would be interesting to see if this is upheld by first-principles calculations. The experimentally observed (Ref. 30) crossover (at trimers) from small Ir clusters preferring hcp binding sites on Ir(111) to large clusters preferring fcc sites could result from the hcp nearest-neighbor bond strength dominating for small clusters and the fcc bond dominating for large clusters. However, it seems more likely to originate from an inversion in the ratio of hcp to fcc site adsorption energies as the adatoms accumulate neighbors.

[19] In Ref. 14, the cluster binding energies were averaged over their values on the fcc and hcp sublattices and, when applicable (Sec. III B), over different cluster orientations before fitting the bond parameters. In this work, only the fcc/hcp averaging is done.

[20] It should be noted that one does nearly as well using the original six bond parameters (''fit'' to only six clusters): the same errors (for 62 clusters) are only (4.2% and 0.63%).

[21] On the other hand, a direct fit to the 62 binding energies gives $u_0 \cong 0.72$ eV with (max., mean) errors of (30.3%, 6.3%). This bond underpredicts the dimer bond by 17% and overpredicts the monolayer bond by 30.3%.

[22] I. J. Robertson, V. Heine, and M. C. Payne, Phys. Rev. Lett. **70**, 1944 (1993).

[23] T. L. Einstein, in *Physical Structure of Solid Surfaces*, edited by W. N. Unertl (Elsevier, North-Holland, 1996).

[24] J. A. Moriarty, Phys. Rev. B **38**, 3199 (1988).

[25] This is probably related to our using mostly bond maximizing cluster geometries (to avoid surface relaxations). For these clusters, the adatom and bulk parameters might tend to occur in only certain combinations.

[26] S. M. Foiles, M. I. Baskes, and M. S. Daw, Phys. Rev. B **33**, 7983 (1986).

[27] On the other hand, assuming $E_{2v}^b = 0.15$ (middle of experimental range), we obtain 10.99 eV for H.

[28] The seven clusters included bond maximizing geometries with two, three (filled), four, five (hollow), six and seven adatoms, and a complete monolayer. Different choices of clusters gave very similar parameters: replacing the monolayer in the previous set with a different (bond maximizing) hexamer gave a maximum change (in A) of 26 meV; whereas, obtaining A from the calculated adsorption energy of a single adatom, G from the mean hollow-filled difference for ''polar'' clusters given in Sec. III B, and the remaining (five) parameters from clusters with two, three, four, five, and seven adatoms gave a maximum change (in E) of 77 meV. The typical change in the parameters for these different cluster choices was about 10 meV. We had much less freedom to choose starting sets than with the six-parameter BSM, as most choices lead again to redundant sets of equations.

[29] For fixed m_0 and m_1, m_2/m_0 differs from the mean square width of N_z, $\overline{(z-\bar{z})^2} = m_2/m_0 - (m_1/m_0)^2$, by a constant. Similar remarks hold for m_3 and the asymmetry, $\overline{(z-\bar{z})^3}$.

[30] S. C. Wang and G. Ehrlich, Surf. Sci. **239**, 301 (1990). The authors observed both linear and triangular trimers (at $T=230$–255 K) with equal probability. They observed a triangular (uppermost in Table I) ground state hexamer which we find to have a binding energy about 0.05 eV smaller than the parallelogram-shaped hexamer in Table II. Similarly, we predict a more elongated 13-adatom ground state than they observed (0.1 eV energy difference).

[31] On the hcp sublattice, the hollow and filled orientations are opposite to those shown in Fig. 3.

[32] M. C. Fallis and C. Y. Fong (unpublished).

[33] R. C. Nelson, T. L. Einstein, S. V. Khare, and P. J. Rous, Surf. Sci. **295**, 462 (1993).

[34] R. K. P. Zia, J. Stat. Phys. **45**, 801 (1986).

[35] W. K. Burton, N. K. Cabrera, and F. C. Frank, Trans. R. Soc. London, Ser. A **243**, 299 (1951).

[36] For details see Refs. 33 and 43.

[37] The size of this vicinity will be determined by how far away from the actual step its presence can be detected. In the BSM, the step can only be ''felt'' by atoms one lattice spacing away (as in Fig. 4) but in reality the step could affect atoms much farther away through a strain field and/or distortion of the nearby electronic charge density.

[38] C.-L. Liu, J. M. Cohen, J. B. Adams, and A. F. Voter, Surf. Sci. **253**, 334 (1991).

[39] The EAM is well known to underpredict these surface energies. See Ref. 26.

[40] As we have discussed, the coordination dependence of interadatom bonds is an *additional* source of multisite (multispin) interactions. These multispin interactions were not treated in Ref. 3.

[41] Because, as discussed in the text, the concept of a microfacet is not really valid for monatomic steps, NEKR's ''awning approximation'' can be ambiguous. However, with it they obtain good estimates of their EAM results for Ag and Pt. Their approxima-tion is in some sense an interpolation scheme, which may explain its accuracy.

[42] M. Breeman, G. T. Barkema, and D. O. Boerma, Surf. Sci. **323**, 71 (1995).

[43] P. J. Feibelman, Phys. Rev. B **52**, 16 845 (1995).

[44] G. Boisvert, L. J. Lewis, and M. Scheffler, Bull. Am. Phys. Soc. **41**, 388 (1996).